

Hypothesis article: A novel strategy to seek bio-signatures at Enceladus and Europa

Philip Judge¹

¹HAO, NCAR*, Box 3000, Boulder CO 80307, USA. judge@ucar.edu

August 27, 2018

Abstract

A laboratory experiment is suggested in which conditions similar to those in the plume ejecta from Enceladus and, perhaps, Europa are established. Using infrared spectroscopy and polarimetry, the experiment might identify possible bio-markers in differential measurements of water from the open-ocean, from hydrothermal vents, and abiotic water samples. Should the experiment succeed, large telescopes could be used to acquire sensitive infrared spectra of the plumes of Enceladus and Europa, as the satellites transit the bright planetary disks. The extreme technical challenges encountered in so doing are similar to those of solar imaging spectropolarimetry. The desired signals are buried in noisy data in the presence of seeing-induced image motion and a changing natural source. Some differential measurements used for solar spectropolarimetry can achieve S/N ratios of 10^5 even in the presence of systematic errors two orders of magnitude larger. We review the techniques and likelihood of success of such an observing campaign with some of the world's largest ground-based telescopes, as well as the long anticipated James Webb Space Telescope. We discuss the relative merits of the new 4m Daniel K. Inouye Solar Telescope, as well as the James Webb Space Telescope and larger ground-based observatories, for observing the satellites of giant planets. As seen from near Earth, transits of Europa occur regularly, but transits of Enceladus will begin again only in 2022.

Keywords: Spectroscopy, spectropolarimetry, life origins

Introduction

In humanity's perennial search for extraterrestrial life, one object seems particularly promising:

“Enceladus has... a textbook-like list of those properties needed for life... [and] the ultimate free lunch: jets that spurt organic material into space” – Catling (2013) [1]

The remarkable story of discoveries about Enceladus by the Cassini Mission and science teams can be found in [2], with post-2013 updates at a JPL webpage¹. Several lines of evidence, including *in-situ* sampling of the ejecta as well as imaging and spectral data, indicate that the plumes contain material similar to that found in hydrothermal vents in Earth's deep oceans (e.g., [3]). To produce properties of some of the ejected rock grains from Enceladus, the water temperature would somewhere have to exceed $\approx 90^\circ\text{C}$. Cassini gas phase CH_4 /hydrocarbon abundance ratios $\sim 10^2$ are compatible with abiotic sources. But these measurements do not reject some production by micro-organisms found on Earth called methanogens (e.g., [1]), which, as extremophile organisms in hydrothermal vent environments on Earth, produce CH_4 /hydrocarbon abundance ratios $\geq 10^3$. This is simply because too little is known about the chemical history of Enceladus,

*The National Center for Atmospheric Research is supported by the National Science Foundation

¹<https://saturn.jpl.nasa.gov/news/2916/cassini-at-enceladus-a-decade-plus-of-discovery/>

and we know nothing about possible biochemical environments there. Europa has three reported episodes of emission of plumes from its interior [4; 5; 6]. Its plume emissions seem to be rare compared with Enceladus.

In the last four decades, research on hydrothermal vent environments has revealed diverse and abundant life forms, living primarily on heat and chemistry. The possible importance of such colonies of non-photosynthetic life for originating all life on Earth has been widely discussed (e.g., [7; 8; 1]). The hydrothermal vents are distributed along the Earth’s tectonic plate boundaries. Tectonic activity is frequently listed as a prerequisite for habitability of planets, continually bringing mineral-rich material to the surface. Some structures on the S. polar surface of Enceladus have been described as “tectonic” [2].

Two classes of vents host very different ecosystems. Most relevant to this paper are the old (at least 30,000 years), alkaline, 90 C vents, typified by the “Lost City Hydrothermal Field” (LCHF) [9]. The vents efficiently release CH_4 and H_2 , unlike their hotter (350 C), acidic “black smoker”, $100\times$ younger counterparts which produce CO_2 , H_2S and some metals. LCHF and black smoker vents support different lifeforms. The LCHF ecosystems are believed appropriate to the Jovian and Saturnian satellites, but at this stage one should not reject out-of-hand the possible importance of the black smokers. In the black smoker ecosystems, microbial organism concentrations are some 10^4 to 10^4 higher than non-venting regions. The LCHF contains of order 10^5 cells cm^{-3} in the LCHF [9; 10], compared with the 3×10^{21} number density of water molecules. We cannot expect to detect directly such cells, but the number densities of much smaller biogenic molecules associated with such cellular life should be much larger.

It seems important to try to detect signs of life in the material ejected from both Enceladus and Europa by whatever means possible. Unfortunately, the earliest planned fly-by and lander will not even launch before 2022, even for Jupiter, pushing back encounters until after 2028. This paper addresses the question, *might we probe this organic material remotely, and attempt to provide the first evidence for extra-terrestrial, simple life?* We will conclude, surprisingly, that we already have in place both the needed instrumentation and techniques to attempt such measurements. However, new laboratory work is also needed to mimic conditions of the water ejected by the satellites into space. So here we put forward a program of research involving extremely high sensitivity imaging spectroscopy, routinely used in solar work, together with some of the most advanced telescope systems on the ground and in space, to attempt such measurements.

Specifically, the ideas expounded here [11] are *to measure, differentially, the absorption spectrum of the plumes as each satellite transits the parent disk*. Such measurements will record dips in the planetary light as both the opaque satellite and the plume material make their disk passages. Circumstances of the transits are listed in Table 1.

Table 1: Circumstances of transits and plumes at Enceladus and Europa, at opposition

Parameter	Unit	Enceladus	Europa
Mean distance (opposition)	km	1.278(9)	6.39(8)
radius	km	257	1480
apparent diameter	arcsec	0.081”	0.97”
cross-plume column density	particles cm^{-2}	1.5×10^{16}	...
plume scale length	km	≈ 100	≈ 500
plume scale length	arcsec	≈ 0.016 ”	≈ 0.16 ”
mean orbital speed	km/s	12.63	13.74
radius/orbital speed	seconds	20.35	107.7
plume scale length/orbital speed	seconds	8	36
maximum transit duration	hours	2.65	2.88
Earliest next transit date		Spring of 2022	...

Data are standard sources, some computed using the JPL ephemeris, and, for plumes, references in the text.

To proceed, we first look at similarities between the transit spectroscopy and solar spectro-polarimetry.

Then we propose laboratory work to see if spectral bio-signatures exist in water sampled from diverse biological habitats in the Earth's oceans. Lastly, we explore the feasibility of the proposed research using some of the world's largest telescopes.

Commonalities with solar spectropolarimetry

These ideas have a superficial similarity to work exploring exo-planetary atmospheres, both use transits and both seek weak signals against a very bright background. But there are significant technical differences: Firstly, exoplanet transits are spatially unresolved, satellite transits must be spatially resolved in order to fill as much of each pixel with plumes; secondly, satellite transits are subject to detrimental seeing-induced noise as images are blurred rapidly in time by Earth's atmosphere; lastly, as the satellite/plume advances across the planetary disk, the background scene is changing in time.

All-in-all, the proposed observations of satellite transits have much more in common with solar work, in particular solar *spectro-polarimetry*, than with the exoplanet transit work. Modern solar observations at visible and infrared wavelengths are generally performed near the diffraction limit using adaptive optics, image reconstruction techniques, and splitting light into both wavelength and polarization states. Several authors (e.g., [12; 13]) have recently reviewed the challenges facing modern solar spectropolarimetry.

The commonalities in the needs for transit spectroscopy and solar spectro-polarimetry are as follows:

- Both require very high signal-to-noise ratios. In the solar case, information on the magnetic field is often encoded in signals as small as 10^{-4} of the measured intensity, in the plumes, the small optical depths and geometric sizes of plume material will lead to similarly small signals of interest.
- The highest angular resolutions possible, close to diffraction limits, are needed in both cases. In the Sun, we try to resolve spatially intermittent magnetic field interacting with plasma at the smallest scales possible, and Enceladus' plumes are a mere 0.016" long, filling a small fraction of the area of the spectrograph slit.
- The small physical scales and rapid changes of the Sun's magnetic field, and of the plumes and their transit across planetary features, both set limits on the largest acceptable exposure times (Table 1).
- Rapid ($\gg 1$ Hz) variations in the seeing conditions. presents a serious problem. Adaptive optics (AO) must be brought to bear because the targets (e.g., sunspots on the Sun, satellites on the planet's disk) show structured objects covering small angular areas.

One advantage presented by satellite plume observations is that, unlike the Sun, we can simply sum all exposures, because we seek an average spectrum. In contrast, modern solar data require integration times of at most seconds to avoid smearing dynamical phenomena of interest. This difference makes up, to some degree, for the much dimmer planetary surfaces.

Needed laboratory work

Transmission spectra of seawater should be obtained in the laboratory, between the atmospheric cutoff at 390 nm and, say 10 μ m, ideally with a resolution $\geq 10^4$. High intensity infrared and visible light sources can be used to obtain transmission spectra through the expanded vapor.

To approach the very low density and pressure conditions at the plumes in space, a sample of liquid water might be made to expand into a vacuum. The number density of water molecules in the plumes can be estimated using the scale lengths of Table 1 and measured column densities of 1.5×10^{16} cm^{-2} [14]. The observed columns [14] are through the jet-like structures, which are of order a factor 10 smaller than the scale lengths in Table 1. Thus, with a path length of around 10 km for Enceladus, we find an average molecular density of water of $n_{H_2O} \approx 1.5 \times 10^{10}$ molecules/ cm^3 .

By most laboratory standards, this is a very low density. Using a sample of say, 0.1 cm^3 of liquid water, which contains $\approx 6 \times 10^{23} \times 0.1 / 18 \approx 3 \times 10^{21}$ molecules, densities inside a vacuum chamber of volume \mathcal{V} cm^3 are $\approx 3 \times 10^{21}/\mathcal{V}$. To produce densities close to those of the plumes would require $\mathcal{V} \approx 2 \times 10^{11}$ or a vacuum chamber of size $L \approx 59$ meters, with a characteristic path length of only $Ln \approx 10^{14}$ molecules cm^{-2} . Instead we consider a vacuum chamber of linear size 1 meter or so, yielding an expanded density $n \approx 3 \times 10^{15}$ cm^{-3} and a column density $nL \approx 3 \times 10^{17}$ cm^{-2} . The latter, which should be high to produce measurable absorption spectra, can be increased by allowing water to expand into an oblate vacuum chamber for the same volume, by factors of the aspect ratio (length/width). By way of comparison, Table 1 lists column density an order of magnitude lower for the Enceladus plumes, which is remarkably close for such diverse conditions. However, post-expansion number densities of H_2O in the vacuum chamber $n \approx 3 \times 10^{15}$ cm^{-3} are 5 orders of magnitude larger than in the plumes, with mean inter-molecular distances of $\Lambda \approx 7 \times 10^{-6}$ cm compared with 4×10^{-4} cm for conditions in Enceladus' plumes. Amino acids contain upwards of a few hundred atoms, each of size 10^{-8} cm, small bacteria are $\geq 10^{-5}$ cm across, prokaryotes $\approx 3 \times 10^{-4}$ cm. In both the plumes and laboratory vessel, any large (biological) molecules or even organisms will be embedded in a very cold and tenuous H_2O vapor, likely with ice particles.

Assuming adiabatic expansion with an exponent of 5/3, the final pressure would approach 0.003 dyne cm^{-2} (a “high vacuum” at $p = 3 \times 10^{-9}$ atmospheres) probably requiring multi-stage pumping with an ion-gauge measurement. The temperature of the vapor in the experiment would be 0.006 K, the mean speed of H_2O molecules 170 cm s^{-1} . With a gas-kinetic cross section of order 10^{-15} cm^2 , we find a collisional mean free path of 0.3 cm and a collision time of 0.002 sec. For isothermal expansion, the collision time would be reduced to 10^{-5} sec and the pressure increased to 10^{-4} atmospheres. The isothermal and adiabatic approximations represent the limits of short and long energy exchange times respectively. In both cases the transmission spectra should be similar since we will be far from sampling optically thick material. The higher number density $\approx 3 \times 10^{15}$ cm^{-3} of laboratory vapor can lead to changes in the spectra of large molecules via “collisions”, because the molecules are packed a factor of 50 closer in the laboratory than in plumes. It is appropriate therefore to vary the densities of the water molecules to look for systematic effects of collisions between any larger molecules and the water vapor substrate.

What kind of water ecosystems should be measured? Known oceanic ecosystems on Earth are based on only two sources of energy (e.g., [15]): sunlight and chemical energy, the second of which was recognized only in 1979 [16]. In the absence of sunlight, deep in the ocean there is abundant life deriving its energy from *chemosynthesis*.

The purpose of the laboratory work is therefore to see if such bio-signatures appear detectable through spectroscopy, for we cannot judge from existing work what signatures might be present. We anticipate performing an experiment along the following lines. A samples of various sources of sea- and fresh-water should be measured differentially against one another. These must include

1. Water from several regions close to hydrothermal vents that are abundant in chemosynthetic life forms, from both high temperature (300 C) acidic (black smoker) and low temperature (90 C) alkaline fumaroles should be examined,
2. Normal seawater,
3. Water from land-surface geysers.

In all cases differential measurements of the same water samples, but with large molecules and organisms removed (by physical and/or chemical means), should be made. The experiment might proceed as follows. A vacuum chamber equipped with a suitable window, and with a volume of $\approx 1 \text{ m}^3$ should be dried and pumped down to less than 10^{-9} atmospheres. A cell containing water samples can be suddenly opened to the vacuum chamber. During this dynamical expansion and relaxation phase, time-resolved spectra should be obtained, using a grating IR spectrometer owing to the small dynamical times of less than a second. Spectra should be obtained prior to and after the rapid expansion phase to allow differential measurements. The experiment can be repeated until sufficient S/N ratios are achieved ($\geq 10^4$). Spectral sensitivity to different pressures and temperatures should be investigated. Finally, it might be that, with the helical handedness of many

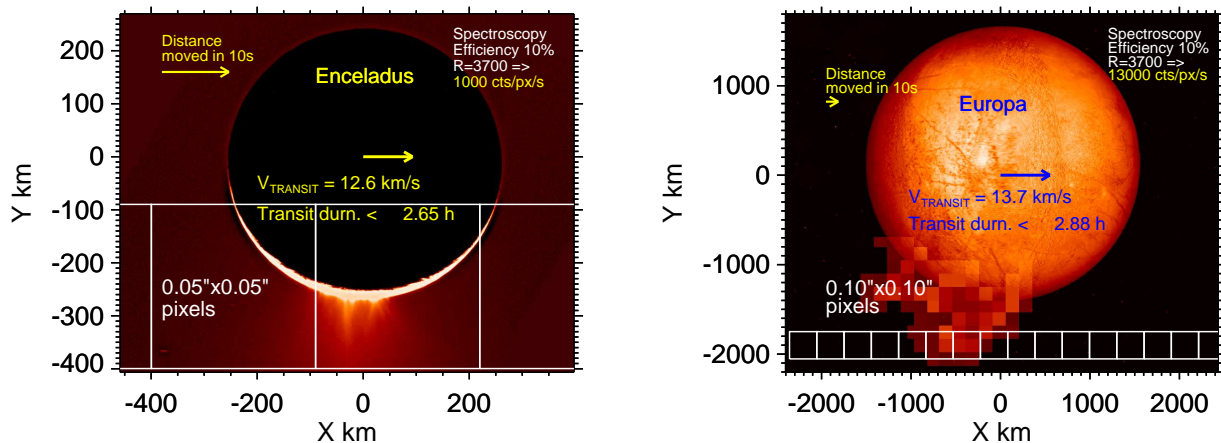


Figure 1: Images of Enceladus (left) and Europa (right) are superposed with data relevant to transits. The images are from NASA's websites.

biomolecules, attempts at circular polarization measurements might be profitable. It is not inconceivable that such measurements will ultimately help us understand the overwhelming bias of life on Earth towards one chirality.

Calculations

Here we will show that the transit measurements proposed are feasible. The question of whether or not *bio*-signatures can be detected depends critically on the outcome of the laboratory work, and on acquisition of the highest possible signal-to-noise ratios of the planets. We proceed in a spirit of scientific exploration of the unknown, assuming that the laboratory work is successful. Here we perform some order-of-magnitude calculations to assess the likelihood of success. We will present Enceladus in detail, showing the experiments to be worthwhile. The numbers in Tables 1 and 2 show that Europa is a far easier target, if it can be caught during a rare episode of ejection of matter.

Figure 1 shows the geometry of transits for the two satellites, together with boxes that represent spatial pixels of angular size $0.05''$ and $0.1''$ that are representative of conditions under which observations appear possible (cf. 2). A balance must be struck between angular resolution and the need to detect plume absorption. While absorption cross sections are high at UV wavelengths, and diffraction-limited angular resolution is also high, UV photon fluxes are very low. Photon fluxes from scattered sunlight from the planetary atmospheres are 3 and 2 orders of magnitude lower at 0.15 and $0.2 \mu\text{m}$ compared with $2 \mu\text{m}$ respectively (using reflectivities from [17]). Estimates (below) of optical depths of even abundant species (such as CH_4) in the plumes show that they will be small, $\tau \approx 10^{-3}$. The signals desired will be a fraction $\approx \tau$ of the intensity. These signals will be diluted further because of the small apparent sizes of the plumes which, for Enceladus, lie below the resolution of most instruments, and for Enceladus and Europa the detrimental effects of atmospheric seeing must be mitigated. A further difficulty for Enceladus is that the velocity of the transiting satellite limits integrations times to, at most, a few seconds (see Table 1), after which the plume intercepts a different part of the planetary surface, and hence surface features, behind it. All of these considerations point to optimal wavelengths between 0.5 and $5 \mu\text{m}$, to find a balance between brightness (which falls rapidly at shorter wavelengths) and angular resolution (diffraction reducing the resolution at longer wavelengths, as $0.24''\lambda[\mu\text{m}]/D[\text{m}]$, D =telescope diameter in m). In the calculations below, we will see that, even at the brightest parts of the spectrum of Saturn and Jupiter, we will be limited by photon noise. Observing between 0.5 and $5 \mu\text{m}$ means that we will be probing signatures of vibration-rotation modes of large molecules. This region contains in principle a variety of spectral bio-signatures (e.g., [18]).

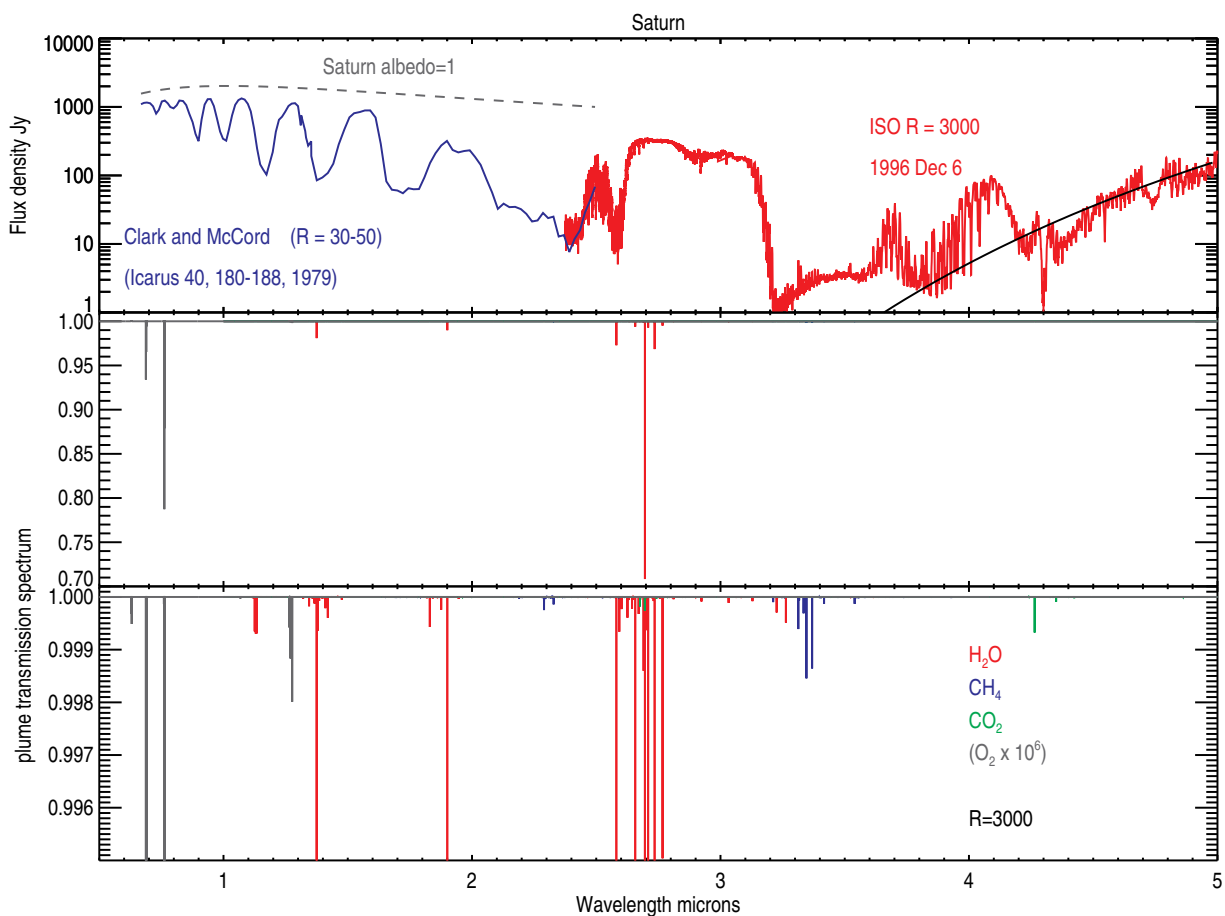


Figure 2: A composite visible-infrared spectrum of Saturn is shown in the top panel. The dashed line shows the brightness of Saturn with a uniform albedo of 1, and the blue line shows a low spectral resolution IR spectrum from [19]. The red curve shows a spectrum from the ISO satellite obtained from the ISO data archive which has a spectral resolution of about 3000. The solid black line is a black body flux spectrum at 174 K from Saturn. The lower panels show spectral transmission calculations for the plumes of Enceladus, scaled differently to reveal strong and weak transitions, computed using the HITRAN database [20] using a spectral resolution of 3000. Other details of the calculations are given in the text.

Signal-to-noise estimates of transmission spectra for Enceladus

First we compute the intensity (brightness) of Saturn between 0.5 and 5 microns, wavelengths at which instruments will operate in space (the James Webb Space Telescope- “JWST”) and on the ground (including DKIST). Several well-known atmospheric transmission windows (the VRI and J-M astronomical bands) allow measurements of astronomical objects from the ground at these wavelengths. Assuming for simplicity that light scattered from Saturn’s cloud decks is uniformly emitted outwards into 2π steradians, the reflected (scattered) light intensity from the planetary surface is

$$I_\nu = \frac{f_\nu}{2\pi} a_\nu \quad \text{erg cm}^{-2} \text{ s}^{-1} \text{sr}^{-1} \text{Hz}^{-1} \quad (1)$$

where a_ν is the planetary albedo at frequency ν , f_ν is the flux density of solar radiation at Saturn (\mathfrak{h}),

$$f_\nu \approx \frac{\pi R_\odot^2}{\Delta_\mathfrak{h}^2} B_\nu(T_\odot) \quad \text{erg cm}^{-2} \text{ s}^{-1} \text{Hz}^{-1} \quad (2)$$

and where $B_\nu(T_\odot)$ is the brightness of the solar disk (here given as a Planck function at $T_\odot \approx 5000\text{K}$). $\Delta_\mathfrak{h}$ is the distance from the Sun to Saturn. Then, retaining the notation $a_\nu B_\nu(T_\odot)$ no matter if the emission is scattering or thermal, recognizing that a_ν is given by the ratio of Saturn’s emission spectrum to the Planck function curve in Figure 2, we have

$$I_\nu \approx \frac{R_\odot^2}{2\Delta_\mathfrak{h}^2} a_\nu B_\nu(T_\odot) \quad \text{erg cm}^{-2} \text{ s}^{-1} \text{sr}^{-1} \text{Hz}^{-1} \quad (3)$$

The flux density from an area on the planet subtending a solid angle ω steradians at a telescope near Earth is simply ωI_ν erg cm⁻² s⁻¹Hz⁻¹. The flux density of photons is just $\omega I_\nu/h\nu$ ph cm⁻² s⁻¹Hz⁻¹, so that for a telescope with an aperture of diameter \mathcal{D} cm², and a total (telescope plus feed optics, spectrograph and detector) system efficiency of photon detection of \mathcal{E} , we find a photon counting rate N_ν (photons Hz⁻¹ s⁻¹) of

$$N_\nu = \frac{\pi}{8h\nu} \frac{R_\odot^2}{\Delta_\mathfrak{h}^2} a_\nu B_\nu(T_\odot) \mathcal{D}^2 \mathcal{E} \omega \quad \text{photons Hz}^{-1} \text{ s}^{-1} \quad (4)$$

It is clear because of the small size of plumes and their large distance that we must make observations close to the diffraction limit of visible and infrared telescopes (Tables 1 and 2). At the diffraction limit the angular size is close to $\vartheta \approx 1.2\lambda/\mathcal{D}$ radians, $\lambda = c/\nu$. If we critically sample the Airy disk using square pixels at the telescope focus where the entrance slit to the spectrograph is placed, we need

$$\vartheta_C \approx \frac{0.6c}{\nu\mathcal{D}} \quad \text{radians.} \quad (5)$$

For a $\mathcal{D} = 4$ meter telescope observing at $4 \mu\text{m}$, $\vartheta_C = 0.12$ arcseconds. Then

$$\omega \approx \vartheta_C^2 = 0.4 \left(\frac{c}{\nu\mathcal{D}} \right)^2 \quad (6)$$

so that the photon counting rate becomes simply

$$N_\nu = \frac{\pi}{4} \frac{R_\odot^2}{\Delta_\mathfrak{h}^2} a_\nu \frac{c^2}{2h\nu^3} B_\nu(T_\odot) \mathcal{E} \quad \text{photons Hz}^{-1} \text{ s}^{-1} \text{Px}^{-1} \quad (7)$$

independent of the telescope aperture, where Px refers to each spatial pixel. Substituting for B_ν in the Rayleigh-Jeans limit we find

$$N_\nu \approx \frac{\pi}{4} \frac{R_\odot^2}{\Delta_\mathfrak{h}^2} a_\nu \frac{kT_\odot}{h\nu} \mathcal{E} \quad \text{photons Hz}^{-1} \text{ s}^{-1} \text{Px}^{-1} \quad (8)$$

For Saturn, at opposition $\Delta_{\text{r}} = 9.53 \text{ A.U.} = 1.43 \times 10^{14} \text{ cm}$. With $R_{\odot} = 6.996 \times 10^{10} \text{ cm}$, the numerical values at $\lambda = 4 \mu\text{m}$ are

$$N_{\nu} \approx 1.8 \times 10^{-7} a_{\nu} \mathcal{E} \text{ photons Hz}^{-1} \text{ s}^{-1} \text{ Px}^{-1} \quad (9)$$

For a spectrograph observing Saturn with resolution $\nu/\Delta\nu = \mathcal{R}$, and critically sampling in wavelength using a detector with spectral pixels S_x with width $0.6c/\nu\mathcal{R}$, we find, for $1 < \lambda < 5 \mu\text{m}$,

$$N_{S_x} \approx 4000 \left[\frac{\lambda}{4\mu\text{m}} \right] \left[\frac{3000}{\mathcal{R}} \right] a_{\nu} \mathcal{E} \text{ photons s}^{-1} \text{ Px}^{-1} \text{ Sx}^{-1}. \quad (10)$$

For Jupiter (4), the numerical constant of 4000 is simply $\Delta_{\text{r}}^2/\Delta_{\text{J}}^2 = 3.4$ times higher. It must also be remembered that Jupiter is closer to Earth (♃) so that potentially any plumes on Europa are far easier to resolve than on Enceladus, for a given ϑ_C and ω (see Figure 1). The above equation allows us to estimate the number of photons per second that can be used for AO correction, using Saturn and the satellite as the source for the AO corrections, noting that $\int N_{\nu} d\nu \approx 10^{15} N_{\nu} \geq 10^6 \text{ photons s}^{-1}$ over the broad visible spectral range. This will give $\geq 10^3$ photons per spatial pixel, when the AO bandwidth is 1 kHz.

As stated above, the values of a_{ν} are simply the ratio of the plotted spectra from [19] and the ISO spectrum shown in Figure 2 to the scaled Planck function to the dashed line, which varies as λ^{-2} at wavelengths longer than those plotted. The brightest “windows” of emission in Figure 2 (broad peaks in the spectrum) all have $a_{\nu} \approx 0.3$, and this value is adopted below, recognizing that other regions of the spectrum will be considerably dimmer.

While the upper panel of Figure 2 represents the background source against which we might attempt to measure the transmission spectrum of the plumes of Enceladus, the lower panels show calculations of the expected transmission of light through the plumes. These calculations include just the abundant molecules found in mass spectrometry work by [21]: H_2O , CH_4 , CO_2 , O_2 . All molecules were assumed to be in the gas phase. [14] showed that Enceladus’s plumes are at least partly in the gas phase. We adopt the relative abundances of [21], H_2O (91%), CH_4 (1.6%), CO_2 (3%), O_2 ($< 1\%$). The H_2O molecular column density was set to $1.5 \times 10^{16} \text{ cm}^{-2}$, determined from transmission spectra of the UV bright star γ Orionis during a flyby of Cassini in 2005, and the plume path length was set to the scale height of the observed plumes, $\sim 10^2 \text{ km}$ [14]. The computed absorption depths of molecular lines are, as expected, roughly in proportion to the molecular abundances. We emphasize several features of Figures 2. Firstly, the dominant absorbers leave plenty of spectral “room” for detection of other molecular species. Secondly, the emission spectrum from Saturn, while spectrally highly structured (Figure 2), offers a bright background ($> 10 \text{ Jy}$) except for the gap between 3.4 and 4 μm . Thirdly, we see that many lines have absorption depths less than 0.001, even though these molecules have relative abundances by number exceeding 1%. In order to perform the proposed experiments it is clear that *we must achieve the highest possible signal-to-noise ratios. Any experiment should try to achieve a sensitivity of better than 10^{-4} of the brightness of the background spectrum of Saturn.* This criterion implies acquiring at least 10^8 photons per spectral range of interest (it could be one spectral pixel or many pixels that all correspond to features discovered in the spectra of water samples on Earth, discussed below).

How to achieve the required signal-to-noise ratios

The transit durations are several hours (Table 1). Using $a_{\nu} \approx 0.3$, a system efficiency $\mathcal{E} \approx 0.3$, we have 400 photons per spectral pixel S_x per spatial pixel P_x per second. This applies to an imaging system critically sampling the diffraction limit, something that is undesirable in solar work owing to limited exposure times on the same solar scene [12; 13], but which is not a problem here as it is only the background scene that is varying during orbital motion. In one transit, this system will accumulate 3×10^6 photons per S_x and per P_x . Given the very small angular sizes of the target plumes, we must avoid binning spatially. We might bin n_s S_x pixels, then we would acquire $3 \times 10^6 n_s$ photons per spectral region of interest per transit. Thus one transit will require $n_s > 36$ to acquire 10^8 photons per spectral element. This can be achieved with a spectral resolution $\mathcal{R} \approx 80$, for example. By observing 10 consecutive transits one could accumulate 10^9 photons

under the same telescope/instrument configuration. The success or failure of this spectral measurement can then be seen to depend critically on the presence of broad features in the samples from the laboratory spectrum.

Thus, photon counting statistics limit the achievable signal-to-noise ratios to the extent that a spectral resolution of 80 appears insufficient, which can only be determined by performing the laboratory experiment. It is likely that systematic errors induced through residual image motions, inaccurate flat-fields and dark currents, instrumental secular changes in sensitivity and other instrumental factors will, uncorrected, limit a set of measurements to far larger systematic noise errors. This is where experience in observational solar physics can help, for ground-based solar data are plagued with similar issues. One of the major problems involves intrinsic and seeing-induced image motion of bright, extended objects, which introduces spurious time-dependent signals from neighboring pixels into the data. Such problems are absent from unresolved sources such as stars, which with care can achieve sensitivities of 10^5 by deep integrations and co-addition of many spectral lines [22]. Yet signal-to-noise ratios on the order of 5×10^3 can be routinely obtained for the Sun [23], sometimes approaching 10^5 [24], even in the presence of rapid image motions. These sensitivities are achieved using a combination of all or some of the following: (1) differential techniques, including split optical beams, beam switching; (2) rapid data acquisition; (3) adaptive optics.

Figure 3 shows an example of how differential measurements might achieve the needed signal-to-noise for the case of transits of Enceladus. While Saturn is over 200 times the diameter of Enceladus, modern telescope systems with AO can correct seeing-influenced images down to rms errors of around 30 mas (the unfilled circle shows a 30 mas radius superposed on the image). The dashed boxes show a 1σ excursion of seeing-induced motions corrected by a good AO system. During an exposure of the spectrograph of order 1-10 seconds, light will enter each of the “pixels” shown from a random distribution of such excursions. Now, let us consider how we might attempt to reach the highest s/n ratios with such measurements.

We wish to recover the absorption spectra of the S. polar plumes which occupy a small area of pixels in Figure 3. We will assume that plumes are present during the entire duration of the transit. Now, pixel $n - 1$ has already been exposed to Saturn’s light through the plumes, some $\Delta t \approx 25$ seconds or so earlier than the image shows, for pixels of size 0.05 arcseconds. Pixel n is, at the time shown, exposed to the plumes, and pixel $n + 1$ has yet to be exposed to the plumes. The time scale of 25 seconds is important for several reasons. On this time scale, we can assume that the underlying light emission by Saturn remains constant, it is modified only by Saturn’s rotation of its cloud belts at the latitude observed. Close to the equator, Saturn’s rotation period is about 10 hours and 14 minutes. Close to the center of Saturn’s disk the cloud decks rotate at roughly 1.6 km s^{-1} , almost 8 times slower than the orbital velocity of Enceladus across the disk, corresponding to $\approx 2.6 \times 10^{-4}$ arcseconds per second, relative to the system’s barycenter when the system is at opposition. For simplicity of exposition here, let us treat Saturn as unchanging during exposures of order 25 seconds or so. (Of course, such corrections will be applied in any final analysis). Then, for each spectral pixel, assuming Saturn’s brightness itself is unchanging, and the instrument is stable, we find that the counts $C_{n\ell}(\tau)$ in spatial pixel n for each spectral pixel ℓ at a time with index τ is given by

$$C_{n\ell}(\tau) = g_{n\ell}I_{n\ell}(\tau) + d_{n\ell}, \quad (11)$$

where $I_{n\ell}(\tau)$ is the intensity imaged on to spectral pixel ℓ at spatial pixel n , averaged over the exposure time centered at time index τ . $I_{n\ell}(\tau)$ includes all of the unknown (except in a statistical sense) seeing-induced and/or instrumental jitter image motions. The detector plus system’s gain is given by $g_{n\ell}$, independent of time index τ (otherwise the detector is a very poor one), and similarly $d_{n\ell}$ is the dark current correction. Now some 20 seconds later, the counts at time index $\tau + 1$ are

$$C_{n\ell}(\tau + 1) = g_{n\ell}I_{n\ell}(\tau + 1) + d_{n\ell}. \quad (12)$$

Subtracting dark currents and dividing these two equations we obtain the ratio of the plume intensity to the non-plume intensity, *for the same region of the planet* simply as follows:

$$\frac{I_{plume}}{I_{non-plume}} = \frac{I_{n\ell}(\tau)}{I_{n\ell\tau+1}} = \frac{C_{n\ell}(\tau) - d_{n\ell}}{C_{n\ell}(\tau + 1) - d_{n\ell}}, \quad (13)$$

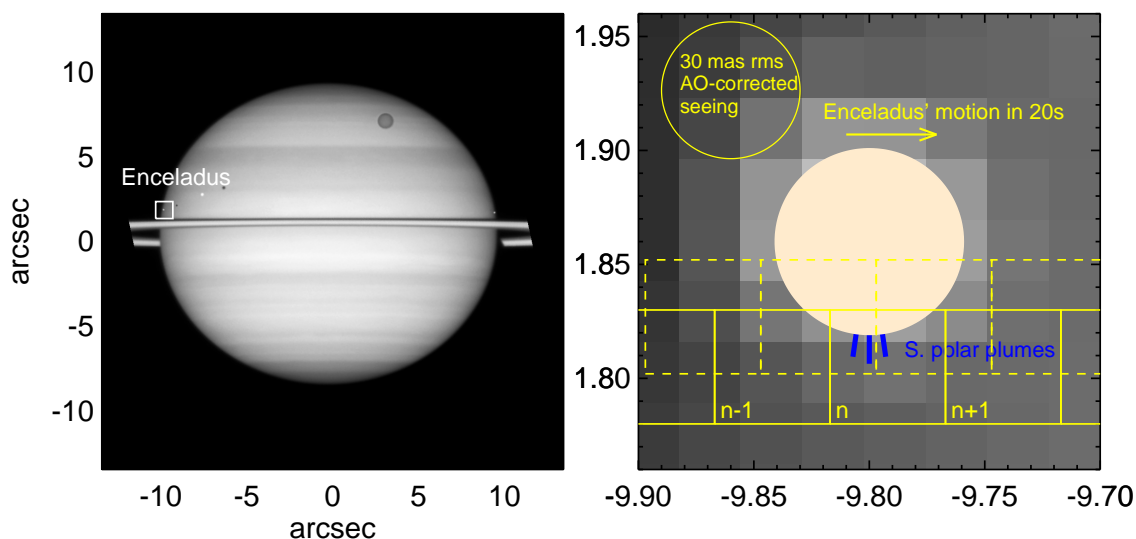


Figure 3: An image of Saturn obtained by the *Hubble Space Telescope* is shown on the left, acquired on February 24th 2009 and obtained from NASA's APOD website <https://apod.nasa.gov/apod/ap090319.html>. Four of Saturn's satellites are captured in various stages of transiting the planet's disk. On the right is a blow up from the small region within the square area in the left panel containing Enceladus (shown as a sharp opaque almond-colored disk superimposed on the highly expanded Hubble image underneath). On this panel (spanning merely 0.2 seconds of arc on a side) a 30 milli-arc-second radius circle is shown representing (optimistically) a good 8m telescope point spread function operating at $\lambda = 1$ micron, after adaptive optical correction. The boxes are $0.05 \times 0.05''$ areas at a hypothetical spectrograph slit oriented E-W on the sky. The dashed box shows a 1σ residual image motion of 30 milli-arcseconds on the sky. (In reality the images will move relative to the fixed spectrograph slit, it is shown in this manner for clarity.)

independent of the gains of each spectral pixel. This manipulation is a trick similar to that used to obtain very high signal-to-noise ratios in stellar spectropolarimetry [22], to avoid dealing with gain corrections. With ≈ 450 such differential measurements for a full transit, we get as before with $\mathcal{R} = 3000$, 3×10^6 photons per spectral and spatial pixel, for both $C_{nl}(\tau)$ and $C_{nl}(\tau + 1)$ respectively. In this case the s/n ratio due to photon statistics would be, assuming changes in dark current are negligible (i.e. using a good detector with $C_{nl}(\tau) \gg d_{nl}$ and $d_{nl} = \text{constant}$ over a few minute period), $\sqrt{2}$ times higher than the noise at one time τ (through the propagation of errors in both $C_{nl}(\tau)$ and $C_{nl}(\tau + 1)$). However, this factor can be reduced to near unity by suitably averaging data for $C_{nl\tau+m}$ for $m = -10$ to $m = +10$ say on the denominator of equation (13), with the assumption that observing conditions do not change in the period of 20 times 20 seconds, a few minutes. Finally, the spectrum desired I_ℓ can be obtained by averaging over all the best exposures.

It seems clear that, sacrificing spectral resolution, and assuming that AO can produce imaging quality with rms seeing of around 30 milli-arc-seconds, the differential measurements represented by the scheme shown in Figure 3 and in equation (13) can get close (≈ 2000) to the desired s/n ratios ($\geq 10^4$) for Enceladus, for just one transit. These techniques are standard in both solar and stellar spectropolarimetry. It should be noted that Enceladus is especially challenging owing to its distance, and relatively small size, which means that modern telescopes cannot resolve the “plumes”. The plume spectra are therefore diluted further by the ratio of the fractional areas of the plume material in each pixel (see Figure 3 for a general idea). In every technical sense, Europa is a far easier target: the surface brightness of Jupiter is larger, the documented plumes are higher, and Europa regularly transits Jupiter’s disk. Signal-to-noise ratios for Jupiter and Europa are larger by a factor of 3.4 (equation 10) and another order of magnitude because the Europa plumes should fill far more of each spatial pixel. Yet its eruptive events appear rare, they are less-well documented. Catling’s “free lunch” [1] has its limits.

A comparison of observatories

In Table 2 we compare relevant IR capabilities of three observatories. Both the JWST and DKIST telescopes are under construction, while Keck telescopes have been in operation since 1993. DKIST is included because, being primarily a solar telescope, it is likely to have less pressure for night-time observations, and because it has interesting capabilities. In particular, the adaptive optics system is designed to vary on a resolved bright source, not on point sources, and it is designed to do full Stokes polarimetry. Enceladus has one of the brightest surfaces in the solar system, and will likely be brighter than Saturn’s disk at the wavelengths considered. One disadvantage of DKIST is the relatively high spectral dispersion of the first-light instrument CRYO-NIRSP, which reduces photon fluxes per pixel. But on the other hand, it is also a coronagraph, which makes it attractive for different kinds of observations of giant planet moons. For example, (see e.g., section 4.2 of [25]) note the need for observations with low stray light while certain moons enter the shadow of their host planet, always very close to the planet itself as seen from Earth.

Let us first consider the ground-based observatories. Referring again to Figure 3 and Table 2, it is easy to see that the spectrum I_{plume} will contain light from Enceladus’ surface during each integration as the residual seeing excursions move the sky image in and out of the spectrograph pixels. For observations from the ground, this contribution must be corrected. Quantifying the contributions to noise is a (relatively) straightforward issue once the brightness gradients between the various objects in the seeing disk are quantified [26; 27], and if the seeing power spectrum is available. Calculations would need to be done if the laboratory experiment succeeds. One major advantage of the transit scenario instead of solar observations is that one can observe Enceladus directly above the limb of the planet prior to and after transit to determine the spectral nature of this contribution. Clearly observations from space, for example from the upcoming James Webb Space Telescope (JWST), can remove seeing-induced contamination when the spacecraft jitter is small enough. The JWST stability requirement (< 3.7 mas) and NIRSpec focal plane geometric distortions (< 10 mas) [28] are sufficient to acquire high quality plume spectra. However, JWST is not ideally suited to such observations, essentially because it was designed for observing much fainter objects, and the pixels under-sample the diffraction limit at the shortest IR wavelengths. This has two obvious consequences: (1) the pixel sizes of the instruments are larger than the plumes, and (2) the larger pixels collect more light, leading to saturation

Table 2: A comparison of three large infrared observatories

Parameter	Unit	DKIST	JWST	Keck II
Primary aperture	m	4	6.5	10
Operations		2019-	2018-	1996-
Diffraction limit at $1\mu\text{m}$	mas*	63	39	25
IR spectrograph		CRYO-NIRSP ⁺	NIRSpec	NIRC-2 Grisms
Minimum pixel size	mas	150	100	10-40
$\mathcal{R} = \lambda/\Delta\lambda$		30,000	2,700	2,500-11,000
AO Strehl ratio [†]		0.3-0.6 [§]	...	0.35 [‡]
Image stability	mas	...	< 3.7	...
maximum slew rate	mas/sec	...	≤ 30	...
Other		Coronagraph, polarimetry	L2 orbit, observations limited to near quadrature [#]	

*Milli-arc-seconds. [†]The Strehl ratio is defined as the peak intensity of a point source divided by the peak intensity of the (theoretical) diffraction-limited point spread function (PSF). If the PSF's have a similar shape, then the rms seeing disk is of order the inverse of the Strehl ratio larger than diffraction. ⁺[30]. [§][31]. [‡][32]. [#][25]. NIRSpec and NIRC-2 data are from instrument web pages, <https://jwst.nasa.gov/nirspec.html> and <https://www2.keck.hawaii.edu/inst/nirc2/genspecs.html>. Note that the 30 mas/sec maximum slew rate for JWST at Jupiter corresponds to $\approx 110 \text{ km s}^{-1}$ at the planet.

of the detectors at least for *imaging* of Jupiter and Saturn's disks. By design, the saturation limits of the NIRSpec *spectrometer* on JWST, operating at its highest dispersion of $\mathcal{R} = 2700$, shown in Figure 2 of [29], lie above the count rates for the expected brightness of all four gas giants in the solar system.

Other observatories have been examined in addition to these examples. The CRIRES spectrometer at the one of the VLT telescopes ($\mathcal{D} = 8.2 \text{ m}$) has $\mathcal{R} = 10^5$ which is rather poorly matched to the much lower spectral resolution required to produce high count rates. The KMOS, NACO and SINFONI instruments on the VLT seem as well suited as the Keck II instrument, the VLT has the MAD multi-conjugate adaptive optics system that has produced $0.09''$ resolution images of Jupiter ². Coronagraphic instruments are less likely to be useful since they introduce seeing-induced variations in brightness in targets such as bright transiting satellites, where the entire scene is bright.

In conclusion, it seems that observatories exist, and will soon come into operation, which can in principle investigate the transmission spectra of plumes of Enceladus. Any plumes detected again on Europa would be far easier targets, should Europa emit additional plumes.

Conclusions

This paper demonstrates the feasibility of making interesting measurements of plumes erupting from the surface of Enceladus, and perhaps Europa. Astronomical and laboratory experiments can and should be performed to try to detect signatures of biological products in the transmission spectra during transits as Enceladus crosses the bright disk of Saturn. The NIRSpec instrument on the JWST can obtain very high quality differential spectra between 1 and $5 \mu\text{m}$, but it has rather large pixels which will dilute the signals of plume material. Ground-based measurements will face the problem of dilution of signals by residual seeing motions on scales larger than the plumes of Enceladus. The situation is different at Jupiter, where any plumes present on Europa are of a much larger physical scale and easier to detect spectroscopically. The problem is, of course, that Europa clearly erupts rarely.

Lastly, since Enceladus' plumes supply Saturn's E ring with material, then similar work when the E

²<https://www.eso.org/public/images/eso0833a/>

ring is close to being "edge-on" but visibly separate from the more massive rings would seem worthwhile. The polarization and perhaps coronagraphic credentials of DKIST might be used to advantage in such observations, as well as observations of giant planet satellites that are in the host planet's shadow. In situations where the desired target lies very close to the very bright planetary disk [25], coronagraphy might be particularly valuable.

I am grateful to Wenxian Li for her comments and interest in the work presented here. The two anonymous referees greatly helped to improve the paper, and the author thanks Carolyn Porco for her thoughts and encouragement.

References

- [1] D. C. Catling. *Astrobiology*. Oxford, 1st edition, 2013.
- [2] J. R. Spencer and F. Nimmo. Enceladus: An Active Ice World in the Saturn System. *Annual Review of Earth and Planetary Sciences*, 41:693–717, May 2013.
- [3] H.-W. Hsu, F. Postberg, Y. Sekine, T. Shibuya, S. Kempf, M. Horányi, A. Juhász, N. Altobelli, K. Suzuki, Y. Masaki, T. Kuwatani, S. Tachibana, S.-I. Sirono, G. Moragas-Klostermeyer, and R. Srama. Ongoing hydrothermal activities within Enceladus. *Nature*, 519:207–210, March 2015.
- [4] L. Roth, J. Saur, K. D. Retherford, D. F. Strobel, P. D. Feldman, M. A. McGrath, and F. Nimmo. Transient Water Vapor at Europa's South Pole. *Science*, 343:171–174, January 2014.
- [5] W. B. Sparks, K. P. Hand, M. A. McGrath, E. Bergeron, M. Cracraft, and S. E. Deustua. Probing for Evidence of Plumes on Europa with HST/STIS. *ApJ*, 829:121, October 2016.
- [6] W. B. Sparks, B. E. Schmidt, M. A. McGrath, K. P. Hand, J. R. Spencer, M. Cracraft, and S. E. Deustua. Active Cryovolcanism on Europa? *ApJL*, 839:L18, April 2017.
- [7] T. Gold. The Deep, Hot Biosphere. *Proceedings of the National Academy of Science*, 89:6045–6049, July 1992.
- [8] T. Gold. *The Deep Hot Biosphere*. 1999.
- [9] W. J. Brazelton, M. O. Schrenk, D. S. Kelley, and Baross J. A. Methane- and sulfur-metabolizing microbial communities dominate the lost city hydrothermal field ecosystem. *Applied and Environmental Biology*, 72:62576270, September 2006.
- [10] C.C. Porco, L. Dones, and C. Mitchell. Could it be snowing microbes on enceladus? Assessing conditions in its plume and implications for future missions. *Astrobiology*, this volume, 2017.
- [11] P. G. Judge. Unpublished poster paper: "Bio-signatures from Enceladus' geysers using transits from 2023". In *Exploring the Universe with JWST II. Science Meeting October 24 - 28, 2016. Montreal, Canada*, October 2016.
- [12] E. Landi Degl'Innocenti. Spectropolarimetry with new generation solar telescopes. *Memorie della Societa Astronomica Italiana*, 84:391, 2013.
- [13] P. G. Judge. Atomic physics and modern solar spectropolarimetry. *Canadian J. Phys*, page in press, 2017.
- [14] C. J. Hansen, L. Esposito, A. I. F. Stewart, J. Colwell, A. Hendrix, W. Pryor, D. Shemansky, and R. West. Enceladus' Water Vapor Plume. *Science*, 311:1422–1425, March 2006.
- [15] C. P. McKay, Porco Carolyn C., T. Altheide, W. L. Davis, and T. A. Kral. The Possible Origin and Persistence of Life on Enceladus and Detection of Biomarkers in the Plume. *Astrobiology*, 8:909–919, October 2008.
- [16] J. B. Corliss, J. Dymond, L. I. Gordon, J. M. Edmond, R. P. von Herzen, R. D. Ballard, K. Green, D. Williams, A. Bainbridge, K. Crane, and T. H. van Andel. Submarine Thermal Springs on the Galapagos Rift. *Science*, 203:1073–1083, March 1979.

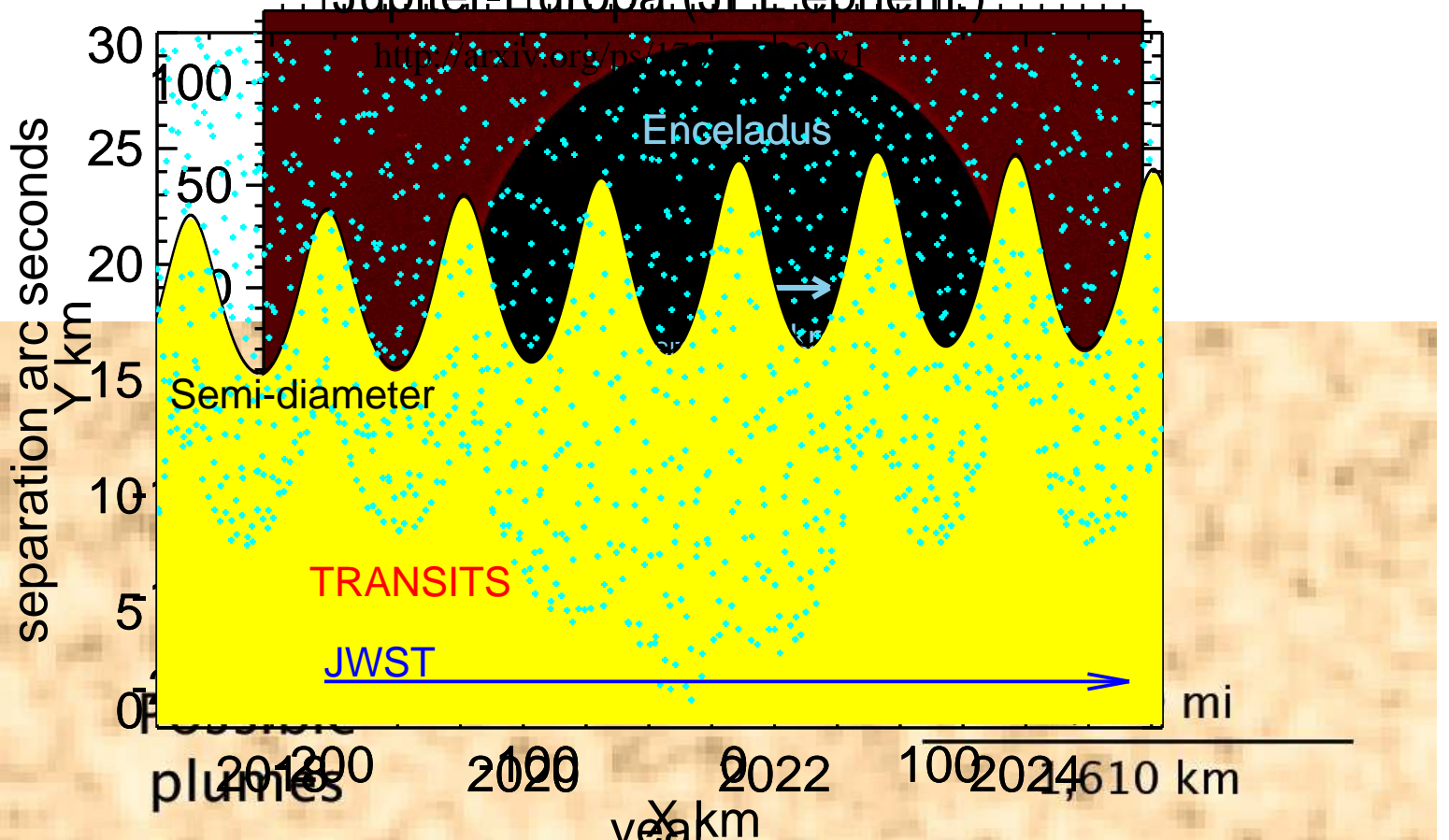
-
- [17] P. F. Morrissey, P. D. Feldman, M. A. McGrath, B. C. Wolven, and H. W. Moos. The Ultraviolet Reflectivity of Jupiter at 3.5 Angstrom Resolution from Astro-1 and Astro-2. *ApJL*, 454:L65, November 1995.
- [18] K. P. Hand, C. F. Chyba, J. C. Priscu, R. W. Carlson, and K. H. Nealson. *Astrobiology and the Potential for Life on Europa*, page 589. 2009.
- [19] R. N. Clark and T. B. McCord. Jupiter and Saturn - Near-infrared spectral albedos. *Icarus*, 40:180–188, November 1979.
- [20] L. S. Rothman, I. E. Gordon, Y. Babikov, A. Barbe, D. Chris Benner, P. F. Bernath, M. Birk, L. Bizzocchi, V. Boudon, L. R. Brown, A. Campargue, K. Chance, E. A. Cohen, L. H. Coudert, V. M. Devi, B. J. Drouin, A. Fayt, J.-M. Flaud, R. R. Gamache, J. J. Harrison, J.-M. Hartmann, C. Hill, J. T. Hodges, D. Jacquemart, A. Jolly, J. Lamouroux, R. J. Le Roy, G. Li, D. A. Long, O. M. Lyulin, C. J. Mackie, S. T. Massie, S. Mikhailenko, H. S. P. Müller, O. V. Naumenko, A. V. Nikitin, J. Orphal, V. Perevalov, A. Perrin, E. R. Polovtseva, C. Richard, M. A. H. Smith, E. Starikova, K. Sung, S. Tashkun, J. Tennyson, G. C. Toon, V. G. Tyuterev, and G. Wagner. The HITRAN2012 molecular spectroscopic database. *JQSRT*, 130:4–50, November 2013.
- [21] J. H. Waite, M. R. Combi, W.-H. Ip, T. E. Cravens, R. L. McNutt, W. Kasprzak, R. Yelle, J. Luhmann, H. Niemann, D. Gell, B. Magee, G. Fletcher, J. Lunine, and W.-L. Tseng. Cassini Ion and Neutral Mass Spectrometer: Enceladus Plume Composition and Structure. *Science*, 311:1419–1422, March 2006.
- [22] S. Bagnulo, M. Landolfi, J. D. Landstreet, E. Landi Degl’Innocenti, L. Fossati, and M. Sterzik. Stellar Spectropolarimetry with Retarder Waveplate and Beam Splitter Devices. *PASP*, 121:993, September 2009.
- [23] M. Collados, A. Lagg, J. J. Díaz Garcí A, E. Hernández Suárez, R. López López, E. Páez Mañá, and S. K. Solanki. Tenerife Infrared Polarimeter II. In P. Heinzel, I. Dorotovič, and R. J. Rutten, editors, *The Physics of Chromospheric Plasmas*, volume 368 of *Astronomical Society of the Pacific Conference Series*, page 611, May 2007.
- [24] A. M. Gandorfer, H. P. P. P. Steiner, F. Aebersold, U. Egger, A. Feller, D. Gisler, S. Hagenbuch, and J. O. Stenflo. Solar polarimetry in the near UV with the Zurich Imaging Polarimeter ZIMPOL II. *A&A*, 422:703–708, August 2004.
- [25] L. Keszthelyi, W. Grundy, J. Stansberry, A. Sivaramakrishnan, D. Thatte, M. Gudipati, C. Tsang, A. Greenbaum, and C. McGruder. Observing Outer Planet Satellites (Except Titan) with the James Webb Space Telescope: Science Justification and Observational Requirements. *PASP*, 128(1), January 2016.
- [26] B. W. Lites. Rotating waveplates as polarization modulators for stokes polarimetry of the sun: evaluation of seeing-induced crosstalk errors. *Applied Optics*, 26:3838–3845, 1987.
- [27] P. G. Judge, D. F. Elmore, B. W. Lites, C. U. Keller, and T. Rimmele. Evaluation of seeing-induced cross-talk in tip/tilt corrected solar polarimetry. *Applied Optics: optical technology and medical optics*, 43, issue 19:3817–3828, 2004.
- [28] B. Dorner, G. Giardino, P. Ferruit, C. Alves de Oliveira, S. M. Birkmann, T. Böker, G. De Marchi, X. Gnata, J. Köhler, M. Sirianni, and P. Jakobsen. A model-based approach to the spatial and spectral calibration of NIRSpec onboard JWST. *Astronomy & Astrophysics*, 592:A113, August 2016.
- [29] J. Norwood, J. Moses, L. N. Fletcher, G. Orton, P. G. J. Irwin, S. Atreya, K. Rages, T. Cavalié, A. Sánchez-Lavega, R. Hueso, and N. Chanover. Giant Planet Observations with the James Webb Space Telescope. *PASP*, 128(1):018005, January 2016.
- [30] A. Fehlmann, C. Giebink, J. R. Kuhn, E. J. Messersmith, D. L. Mickey, I. F. Scholl, D. James, K. Hnat, G. Schickling, and R. Schickling. Cryogenic near infrared spectropolarimeter for the Daniel K. Inouye Solar Telescope. In *Society of Photo-Optical Instrumentation Engineers (SPIE) Conference Series*, volume 9908 of *Proc. SPIE*, page 99084D, August 2016.
- [31] L. C. Johnson, K. Cummings, M. Drobilek, S. Gregory, S. Hegwer, E. Johansson, J. Marino, K. Richards, T. Rimmele, P. Sekulic, and F. Wöger. Solar adaptive optics with the DKIST: status report. In *Adaptive Optics Systems IV*, volume 9148 of *Proc. SPIE*, 2014.
-

- [32] M. A. van Dam, A. H. Bouchez, D. Le Mignant, E. M. Johansson, P. L. Wizinowich, R. D. Campbell, J. C. Y. Chin, S. K. Hartman, R. E. Lafon, P. J. Stomski, Jr., and D. M. Summers. The W. M. Keck Observatory Laser Guide Star Adaptive Optics System: Performance Characterization. *PASP*, 118:310–318, February 2006.

This figure "placeholder.jpg" is available in "jpg" format from:

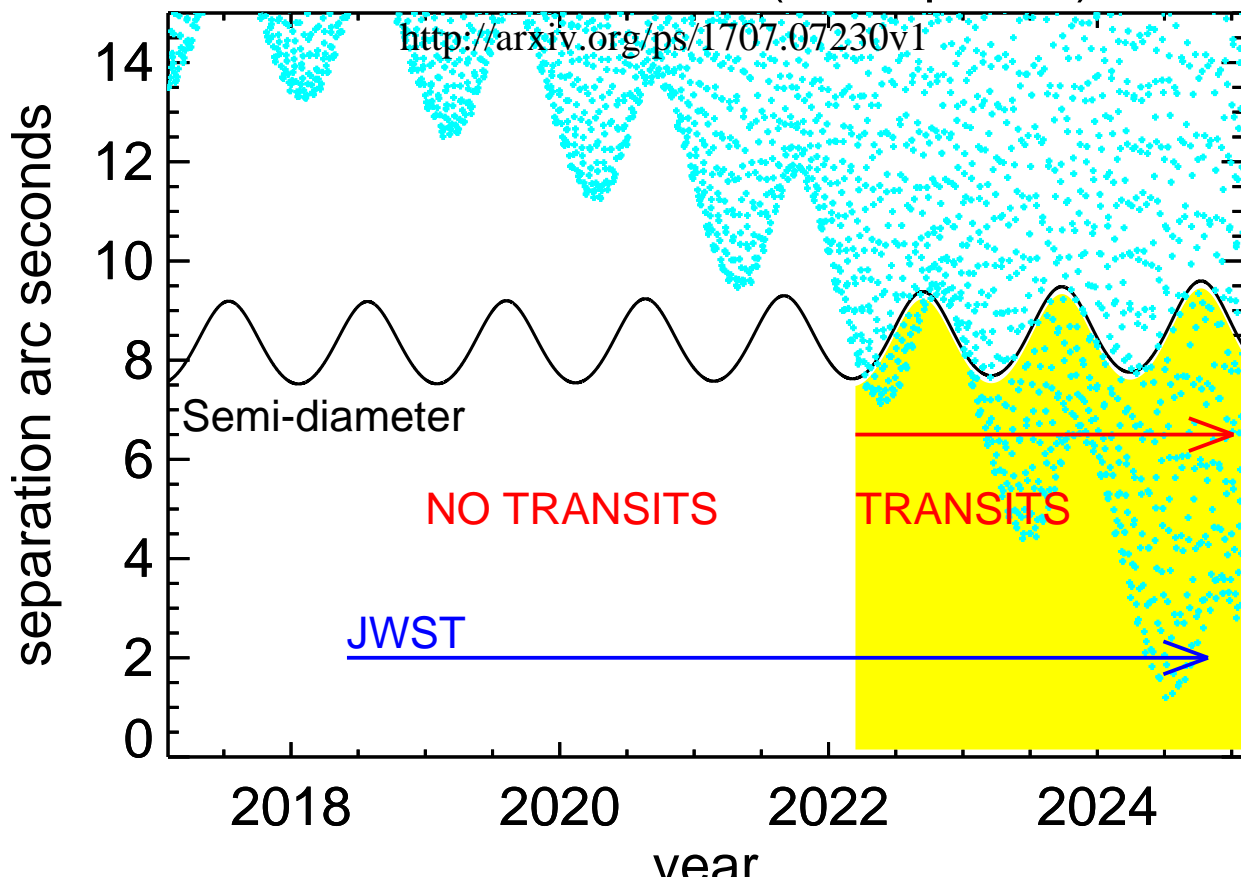
Jupiter-Europa (JPL_ephem.)

<http://arxiv.org/ps/1708.02901>



This figure "stream.jpg" is available in "jpg" format from:
Saturn-Enceladus (JPL ephem.)

<http://arxiv.org/ps/1707.07230v1>



This figure "waite08f1.jpg" is available in "jpg" format from:

<http://arxiv.org/ps/1707.07230v1>